Published in final edited form as:
J Neurosci Res. 2014 April ; 92(4): 531–541. doi:10.1002/jnr.23332.

Characterization of Thoracic Motor and Sensory Neurons and Spinal Nerve Roots in Canine Degenerative Myelopathy, a Potential Disease Model of Amyotrophic Lateral Sclerosis

Brandie R. Morgan[a], **Joan R. Coates**[c], **Gayle C. Johnson**[d], **G. Diane Shelton**[e], and **Martin L. Katz**[b,*]

[a] Department of Biological Sciences, University of Missouri, Columbia, Missouri USA 65211

[b] Mason Eye Institute, University of Missouri School of Medicine, Columbia, Missouri, USA 65212

[c] Department of Medicine and Surgery, University of Missouri College of Veterinary Medicine, Columbia, Missouri, USA 65211

[d] Department of Veterinary Pathobiology, University of Missouri College of Veterinary Medicine, Columbia, Missouri, USA 65211

[e] Department of Pathology, School of Medicine, University of California San Diego, La Jolla, CA 92093-0709

Abstract

Canine Degenerative Myelopathy (DM) is a progressive adult-onset multisystem degenerative disease with many features in common with amyotrophic lateral sclerosis (ALS). As with some forms of ALS, DM is associated with mutations in superoxide dismutase 1 (*SOD1*). Clinical signs include general proprioceptive ataxia and spastic upper motor neuron paresis in pelvic limbs, which progress to flaccid tetraplegia and dysphagia. The purpose of this study was to characterize DM as a potential disease model for ALS. We previously reported that intercostal muscle atrophy develops in dogs with advanced stage DM. To determine if other components of the thoracic motor unit (MU) also demonstrated morphological changes consistent with dysfunction, histopathologic and morphometric analyses were conducted on thoracic spinal motor neurons (MN) and dorsal root ganglia (DRG), and in motor and sensory nerve root axons from DM-affected Boxers and Pembroke Welsh Corgis (PWCs). No alterations in MNs, or motor root axons were observed in either breed. However, advanced stage PWCs exhibited significant losses of sensory root axons, and numerous DRG sensory neurons displayed evidence of degeneration. These results indicate that intercostal muscle atrophy in DM is not preceded by physical loss of the motor neurons innervating these muscles, or of their axons. Axonal loss in thoracic sensory roots and sensory nerve death suggest sensory involvement may play an important role in DM disease progression. Further analysis of the mechanisms responsible for these morphological findings would aid in the development of therapeutic intervention for DM and some forms of ALS.

[*]Corresponding author at: Martin L. Katz University of Missouri School of Medicine Mason Eye Institute One Hospital Drive Columbia, Missouri, 65212, USA katzm@health.missouri.edu (M. Katz).

Keywords

SOD1; dog; axon; morphometry; dorsal root ganglion

Introduction

Canine degenerative myelopathy (DM) is a hereditary neurodegenerative disorder with onset of clinical signs occurring in dogs 8 years or older (Averill 1973). Clinical signs appear in pelvic limbs as spastic upper motor neuron (UMN) paresis and general proprioceptive ataxia, which progresses to flaccid tetraplegia and dysphagia if euthanasia is delayed (Coates and Wininger 2010). Like some forms of familial amyotrophic lateral sclerosis (ALS) DM is associated with mutations in *SOD1* (Andersen et al. 1996; Coates and Wininger 2010; Morgan et al. 2013). DM occurs in many breeds and is typically accompanied by the *SOD1* missense mutation *SOD1:c.118G>A*, which predicts a p.E40K substitution (Awano et al. 2009). The clinical signs, disease progression, and muscle pathology in DM are similar to those seen in some forms of human *SOD1*-ALS. Thus it appears that DM may potentially be a good disease model for some types of ALS.

In ALS patients who receive extensive palliative care, death usually results from failure of respiratory muscle function, typically within 3-5 years after clinical onset. While many ALS patients are medically managed and survive for relatively long periods in severely debilitated states with respiratory and feeding assistance, DM affected dogs are usually euthanized at earlier disease stages when signs progress to nonambulatory paraparesis or paraplegia. However, some DM-affected dogs are maintained until respiratory dysfunction develops (Ogawa et al. 2011; Ogawa et al. 2013). Therefore, both ALS and DM are characterized by the occurrence and progression of UMN and lower motor neuron (LMN) signs, which ultimately result in flaccid tetraplegia and respiratory failure (Brooks et al. 2000; Coates and Wininger 2010; Ogawa et al. 2011; Ogawa et al. 2013) (Table III). Histopathological similarities between DM and ALS include myelinated axon loss and gliosis within the spinal cord, myelinated axon loss in peripheral nerves and muscle atrophy. Accumulations of cytoplasmic aggregates containing SOD1 within motor neurons (MNs) also occurs in DM and some forms of ALS (Andersen et al. 1996; Awano et al. 2009; Charcot J-M 1869; Forsberg et al. 2010; Hirano 1991; Shelton et al. 2012; Sobue et al. 1987; Morgan et al. 2013; Averill 1973; Giannini et al. 2010)). Although ALS is generally considered primarily a disease of the motor system, in some cases there is growing evidence indicates sensory involvement (di Trapani et al. 1986; Dyck et al. 1975; Guo et al. 2009; Heads et al. 1991; Isaacs et al. 2007; Kawamura et al. 1981; Mulder et al. 1983; Pugdahl et al. 2007). Sensory deficits are also characteristic features of DM (Averill 1973).

Although the degenerative changes in the spinal cord neuronal fibers have been known for some time (Griffiths and Duncan 1975; Averill 1973), LMN involvement in DM is a relatively new finding (Awano et al. 2009; Coates et al. 2007; Shelton et al. 2012; Morgan et al. 2013; Ogawa et al. 2013). We recently reported that intercostal and pelvic limb muscles from Pembroke Welsh Corgis (PWCs) at late stage disease exhibited marked pathological changes consistent with denervation atrophy (Morgan et al. 2013; Shelton et al. 2012). Also,

thoracic MNs that innervate the intercostal muscles contain cytoplasmic aggregates that stain with an anti-SOD1 antibody (Awano et al. 2009; Morgan et al. 2013). The degenerative changes in the intercostal muscles suggest that thoracic motor units are dysfunctional in DM, and may result from impaired MN input to these muscles. In most forms of ALS loss of spinal MNs and axonal degeneration are considered disease hallmarks (Hirano 1991; Sobue et al. 1981), and loss of MN input appears to play an important role in the pathology that develops in the associated muscles. To assess whether the thoracic muscle atrophy in DM is also associated with MN defects, morphometric analyses were performed on thoracic MNs and motor axons from DM-affected dogs and age-matched control dogs. In addition, evaluations were performed to determine whether DM is accompanied by alterations in the thoracic sensory nerves and their axons.

Materials and methods

Tissue collections from dogs

Tissues were obtained from companion dogs between 2009 and 2013. Samples were acquired from 14 Boxers (6 control ages 8 to 12 years; and 9 DM-affected ages 10 to 12 years) and 21 Pembroke Welsh Corgis (PWCs) (7 control, ages 13 to 17 years; and 15 DM-affected, ages 12 to 15 years) (Table I). Dogs were diagnosed with presumptive DM at academic, private specialty or general practices based on clinical presentation and progression of upper motor neuron and lower motor neuron signs, and general proprioceptive ataxia that began in the pelvic limbs (Coates and Wininger 2010). Histopathological evaluations of the thoracic spinal cords were performed on all of these dogs. Only those dogs that had exhibited clear clinical signs of DM, and thoracic spinal cord lesions characteristic of this disease (Averill 1973) were designated as DM-affected. Control tissue was obtained from age and breed matched unaffected dogs euthanized for causes unrelated to DM. Dogs were designated as controls if they had not exhibited clinical signs of DM and histological appearance of the thoracic spinal cord tissue was normal. Dogs that exhibited clinical signs similar to those of DM were excluded if their clinical signs were associated with spinal cord compressive lesions detected by magnetic resonance imaging or myelography or if the thoracic spinal cord histopathology was not typical for a diagnosis of DM [(Coates and Wininger 2010).

Genotypes at canine *SOD1:c.118G>A* were determined for each dog included in the study using a TaqMan^{TM} allelic discrimination assay that employed *5'-GTGGGCCTGTTGTGGTATCA-3'* with *5'-CAAACTGATGGACGTGGAATCC-3'* for the PCR primers and *5'-VIC-CTCGCCTTTAGTCAGC-MGB-3'* (*A* allele) and *5'-FAM-CGCCTTCAGTCAGC-MCB-3'* (*G* allele) for the completing probes (Awano et al. 2009). The classification of the dogs by disease status and genotype is shown in Table II.

When an owner elected to have a dog euthanized, the veterinarian who would perform the necropsy was provided with a kit that included detailed instructions and materials for sample collection, preservation and shipping. Detailed clinical histories were obtained to document the age at onset and progression of clinical signs, neurologic status at the time of euthanasia, and any unrelated health problems. Necropsies were performed within 6 hours after euthanasia. Protocols for tissue collection were approved by the University of Missouri

Animal Care and Use Committee. Tissues collected included thoracic spinal cord segment 6 (T6) fixed in buffered 10% formalin, the T7 segment fixed in 3.5% paraformaldehyde with 0.1% glutaraldehyde and 120 mM sodium cacodylate, 1 mM $CaCl_2$, pH 7.4 (Immuno-fixed), and the T8 segment (with ventral and dorsal roots, and dorsal root ganglion intact) fixed in 2% glutaraldehyde, 1.12% paraformaldehyde, 130 mM sodium cacodylate, 1 mM $CaCl_2$, pH 7.4 (electron microscopy [EM]-fix). Blood samples for DNA isolation were collected in EDTA vacutainer tubes (Becton Dickenson, catalogue #367899).

Disease status determinations

Confirmation of disease status for each dog was performed as previously described (Morgan et al. 2013). Briefly, disease stages at time of euthanasia were determined using a clinical grading scale (Table III) (Shelton et al. 2012). DM diagnoses were confirmed histopathologically by assessing the T6 cord segment for evidence of myelinated axon loss and pronounced astrogliosis in the dorsal portion of the lateral funiculus (Averill 1973; March et al. 2009). Dogs that had exhibited clinical signs of DM but did not show the typical histopathology were presumed to have another cause for the myelopathy and excluded from the study. T7 spinal cord segments were examined for the presence of SOD1 immunoreactive aggregates within ventral horn motor neurons (Awano et al. 2009). Dogs that had not exhibited any clinical signs of DM prior to euthanasia and whose thoracic spinal cords were histologically normal were used as controls. Tables I and II provide a summary of the disease status of the dogs employed in this study.

Spinal cord motor neuron cell body counts

An immuno-fixed T7 spinal cord segment from each dog was embedded in paraffin. From each paraffin-embedded sample, 4μm sections (each separated by at least 100μm) were placed on positive charged slides (1 section per slide), and left flat on a 43°C slide warmer overnight. The slide-mounted sections were steam-treated in a decloaking chamber (Biocare Medical, Concord,CA.) at 98°C for 30 minutes in citrate target retrieval solution (Dako, Carpinteria, CA.), cooled at room temperature for 10 minutes, rinsed with distilled water, then placed on IntelliPATH FLX autostainer for staining. Slides were treated with 3% H_20_2 for 15 minutes, washed in buffer, treated with Sniper block (Biocare Medical, Concord, CA.) for 20 minutes. They were then incubated in primary antibody goat anti-choline acetyl transferase (ChAT) (Millipore AB144P;1:200) for 60 minutes. Control sections were treated with nonimmune rabbit IgG (Sigma, St. Louis, MO.) at a 1:1000 dilution for 60 minutes in place of the anti-ChAT antibody. The detection system used was rabbit anti-goat horse radish peroxidase (HRP) kit (PK6105;Biocare Medical, Concord, CA.) with 30 minute incubations in link and label steps followed by a tris buffer rinse. The sections were then incubated in romulin red (Biocare Medical, Concord, CA.) for 10 minutes. Slides were counterstained in hematoxylin (Biocare Medical, Concord CA.) at a 1:10 dilution for 5 minutes then followed with a tris-buffered rinse, dehydrated, coverslipped, and then imaged with light microscopy at 200x magnification. The numbers of ChAT-positive cell bodies in Rexed lamina 9 per section were determined by counting the cells in a sufficient number of sections from each spinal cord sample such that a minimum of 100 cells per dog were counted. Using Image J™ software, cross-sectional area (CSA) was determined for all

ChAT-positive cells in Rexed lamina 9. CSA and diameter of motor neurons with visible nucleoli were also determined.

Morphometric and pathologic analyses of nerve roots

Approximately 3 mm long segments of ventral and dorsal roots were dissected from the EM-fixed T8 cord segments. The samples were post-fixed with 2% osmium tetroxide and subjected to extended microwave infiltration and embedded in epon araldite resin. After resin embedding, blocks were polymerized at 60°C for 48 hours, and nerve cross-sections were cut at a thickness of 0.4μm. The sections were stained in 2% P-phenylene diamine (PPD) solution (MP Biomedicals, LLC, catalog # 151830) (1g PPD in 50ml of 50% EtOH) made up 5 days to 2 weeks prior to use. Sections were incubated in filtered PPD solution for 15 minutes, rinsed 1-3 times in ultra-pure H_2O, covered with Permount mounting medium and coverslipped. High resolution images of each stained nerve cross section were obtained using a Leica DMI 6000B inverted scope equipped with a programmed stage and Leica application suite advanced fluorescence software™ (LAS-AF). Using automated stage controls and image acquisition individual images totaling the entire area of each section were obtained using a 40X objective and stitched together by the LAS-AF software to create a single high-resolution image of the tissue cross section. The sharpness and contrast of the composite images were optimized using Photoshop™ software. The resulting images were then analyzed using MetaMorph® image analysis software to obtain the following morphometric data for each nerve: total myelinated axon number, endoneurial area, endoneurial area occupied by axons, percent axon occupancy (percentage of endoneurial space occupied by myelinated axons), axon density, and axon size distribution. The image analysis procedure is summarized in figure. 1.

PPD and toluidine blue stained sections of the motor roots were examined for histopathogical abnormalities by an experienced pathologist (GDS) in a masked manner. Fibers with inappropriately thin myelin sheaths relative to axon diameter, myelin splitting and ballooning, axonal degeneration and number of probable regenerating clusters (defined as two or more closely apposed myelinated fibers) were assessed in each nerve specimen. As previously described (Shelton et al. 2012), only those fibers with clear, faintly staining space evident between separated myelin with an asymmetrical profile are considered to have splitting and ballooning, while profiles containing paranodal regions or Schmidt-Lanterman clefts were not counted.

Statistical analyses

Data for each breed was evaluated independently. Each data set was evaluated for normality using the Shapiro-Wilk normality test. For data that were normally distributed Student's *t*-test was employed to determine whether significant changes exist between affected and unaffected groups. When data were analyzed using disease stage (early and late) as a variable, data were subjected to analysis of variance followed by Holm-Sidak analyses to compare individual groups. Data that were not normally distributed were analyzed using the Mann-Whitney ranked sum test.

Results

T7 motor neuron density and morphology

DM did not result in significant changes in mean motor neuron densities or mean cell body cross-sectional areas of the T7 spinal cord segment for either breed compared to controls, even when data for all affected dogs within each breed were pooled (Figure 2.C), or when control samples were compared only to late stage DM samples (data not shown). Although DM did not appear to affect the mean size of the T7 motor neuron cell bodies, the disease was associated with increased variability in neuron size in the PWCs (Figure 2.C). This difference is attributed to the motor neurons from late stage PWC compared to those of unaffected PWC ($p= 0.04$), indicating an increased variability in motor neuron cell body size in late stage dogs. In some affected and unaffected samples of both breeds motor neuron morphological abnormalities (i.e. vacuoles, eccentric nuclei, and shrinkage) were occasionally seen, with no apparent correlation with disease status (Figure 2B).

No disease related changes were seen in ventral root motor axons

Among Boxers and PWCs, DM was not associated with significant alterations in the motor root features that were analyzed relative to age-matched unaffected dogs, even in dogs in the most advanced stages of clinical disease (Tables IV and V). Total numbers of axons in the motor roots were similar between affected and normal dogs within each breed. Among both normal and affected dogs, the Boxers consistently had larger numbers of axons in the thoracic motor roots than did the PWCs (Tables IV and V). Additionally, when data were separated into early and late stage groups within each breed, no significant differences were detected in any morphometric measurements compared to control unaffected motor roots (data not shown). Size distribution histograms reveal a bimodal distribution of axon diameters typical of thoracic ventral roots (Figure 3). The smaller caliber peak (≤ 5 microns) represents axons of autonomic neurons from the intermediate substance nuclei (Sobue et al. 1981). The larger caliber peak (>5 microns) likely represents alpha motor axons (Braund et al. 1982). There were no differences in the relative distribution of axons between these two size classes between samples from unaffected and affected dogs (Figure 3). Histopathologic changes including myelin pathology, axonal degeneration, and presumptive regenerative clusters were present in control and affected samples from both breeds. Since no apparent correlation with disease was noted, these changes likely represent features of normal aging or may also include postmortem artifacts.

Significant axonal loss in T7 dorsal roots of DM-affected Pembroke Welsh Corgis

Late stage DM (grades 3 and 4) was accompanied by an average 23% reduction in the number of T7 dorsal root axons of PWC's (unaffected: 3,261 ± 354, affected: 2,498 ± 324, $p = 0.003$) (Figure 4 and 5); however, no differences were seen in the other morphometric measurements including average endoneurial cross sectional area, average area occupied by axons, % of endoneurial area occupied by axons, and average axon density (Table VI). The axons in the sensory roots also exhibited a bimodal distribution in axon diameters (Figure 5). The disease-related decrease in axon number in sensory roots was seen in both large (>5μm) and small (≤ 5 μm) size classes (Figure 5). Morphological features indicative of myelin pathology and axonal degeneration were not disease-associated (data not shown). Among

the affected PWCs, the dorsal root ganglia (DRGs) had large numbers of cells with dark condensed cytoplasm and pyknotic nuclei (Fig. 4D) which were not seen in DRGs from age-matched unaffected dogs (Fig. 4C).

Discussion

Substantial atrophic changes occur in the intercostal muscles in DM prior to the onset of clinically evident impairment in respiratory function (Morgan et al. 2013). Despite clear evidence of intercostal muscle atrophy, no alterations in the numbers of thoracic spinal motor neurons nor in their associated axons were observed in the affected dogs. Likewise, we previously reported that there was no evidence of denervation of the intercostal muscle acetyl choline receptor complexes in DM prior to respiratory impairment (Morgan et al. 2013), unlike the denervation reported in some putative mouse models of ALS (Dadon-Nachum et al. 2011; Fischer et al. 2004; Schaefer et al. 2005). These data indicate that intercostal muscle atrophy in DM is not secondary to loss of physical contact with motor neurons.

All of the dogs evaluated in this study were euthanized prior to reaching end-stage (terminal) disease when respiratory failure would occur. In the United States, from which we obtained all of our samples, owners usually will not maintain their dogs until terminal disease stage when respiratory signs become apparent. We have collected necropsy samples from over 200 DM-affected dogs of various breeds and all have been euthanized prior to exhibiting clinically apparent respiratory signs. As a consequence, it was not possible for us to study thoracic motor neurons and associated muscles from dogs at terminal stage disease that corresponds to the stage at which most samples for histopathological analysis are obtained from human subjects with ALS. However, due to differences in cultural norms, some owners of affected dogs in Japan do maintain affected dogs until very late stage disease when respiratory impairment occurs. Ogawa et al. reported that PWCs at this stage of the disease did exhibit significant loss of motor neurons in the thoracic cord (Ogawa et al. 2013). By comparing the data of Ogawa et al. at terminal disease to our data on dogs are earlier stages of disease progression, we can conclude that the muscle atrophy we reported in affected dogs (Morgan et al. 2013) precedes the degeneration of thoracic cord motor neurons.

These findings are consistent with a study by Wong and Martin in which they domonstrated that skeletal muscle-restricted expression of human mutant SOD1 causes muscle atrophy followed by secondary motor neuron degeneration in mice (Wong and Martin, 2010). Direct effects of *SOD1* mutations on skeletal muscle that could lead to secondary motor neuron degeneration include impairment of muscle mitocondrial function (Zhou et al. 2010). It is also possible that the intercostal muscle atrophy that precedes motor neuron degeneration is due at least in part to functional defects in the motor neurons that are not reflected in obvious structural changes in the nerves. Functional defects in the motor unit that have been reported to precede neuronal soma degeneration in ALS and other neuromuscular diseases include defects in axonal transport, mitochondrial dysfunction, RNA processing, and neurotrophin signaling (Katsuno et al. 2012; King et al. 2011; Redler and Dokholyan 2012;

Shi et al. 2010; Tanaka et al. 2012). Motor neuron function may also be impaired by alterations in synaptic input from cortical and brain stem neurons (Sunico et al. 2011).

The loss of thoracic sensory root axons and degenerative changes in DRG neurons are consistent with a previous report of similar DM-associated sensory nerve pathology (Griffiths and Duncan, 1975), although the degenerative changes we observed in the neurons of the DRG were more profound than the mild central chromatolysis previously reported (Griffiths and Duncan, 1975). Although clinical signs of DM and ALS are primarily associated with motor dysfunction, sensory deficits are also known to occur as part of the clinical spectrum of both diseases (Andersen et al. 1996; Andersen et al. 1995; Averill 1973; Coates and Wininger 2010; Dyck et al. 1975; Isaacs et al. 2007; Mulder et al. 1983; Pugdahl et al. 2007). For example, symptoms of sensory dysfunction in patients with some forms of ALS have been reported to include numbness in the legs and a burning sensation in the feet, decreased light touch and pinprick sensation, reduced vibration sense, and reduced laryngeal sensation. Additionally, sensory fiber loss has been reported in sural nerves (di Trapani et al. 1986; Giannini et al. 2010; Heads et al. 1991; Isaacs et al. 2007), and dorsal roots (Kawamura et al. 1981) in familial and sporadic ALS patients and in transgenic *SOD1* rodent models (Guo et al. 2009). The general proprioceptive ataxia and dorsal column degeneration in DM parallels the sensory dysfunction in some types of ALS. Based on clinical signs and pathologic findings within the disease spectrum of ALS, sensory involvement may represent a variant of the disease or a continuum of a multi-system degenerative disease process (Heads et al. 1991). Our data indicating that significant loss of sensory neurons precedes any physical loss of motor neurons in the thoracic spinal cord suggests that more thorough investigation of the potential role of sensory pathology in ALS is warranted.

The function of the motor neurons innervating the intercostal muscles is dependent at least in part on a feedback loop that involves the sensory neurons from the same cord segment. It is possible that the early pathology exhibited by the thoracic cord sensory neurons results in secondary abnormal function of the motor neurons they innervate and thereby is involved in the early stages of intercostal muscle atrophy (Ausborn et al. 2009; Mentis et al. 2011). Indeed, in some neuromuscular disorders, sensory impairment precedes motor dysfunction (Vucic et al. 2012). In diseases like DM and ALS deficits in sensory functions that are subconscious, such as those involved in regulating respiration, would be difficult to detect.

Our findings, in conjunction with those of Ogawa et al (2010) and Zhou et al (2010) indicate that for the intercostal muscles, muscle atrophy and sensory neuron degeneration precede the degeneration of the associated motor neurons. Whether this is the case for other motor units in DM remains to be determined. Examination of the hind limb muscles of the same dogs used in this study indicated that muscle degeneration was accompanied by degeneration of the associated nerves (Shelton et al 2012). However, at the points the dogs were euthanized, hind limb pathology was well advanced, so it was not possible with the samples available to determine whether muscle atrophy preceded nerve degeneration. In DM, hind limb involvement precedes fore limb involvement. Some dogs are euthanized after exhibiting only hind limb involvement, whereas others are maintained until the fore limbs are also affected clinically. This is particularly true of PWCs. Therefore, it should be possible to

collect fore limb muscle samples and associated spinal cord regions from affected PWCs at various stages of disease progression to determine whether the muscle atrophy and sensory neuron degeneration precedes motor neuron degeneration in other motor units. Such studies will be important to determine whether the same mechanisms underlie muscle atrophy and lower motor neuron degeneration for all regions of the neuromuscular system.

Every PWC and Boxer in which DM has been confirmed, both on the basis of clinical signs and the presence of characteristic pathological lesions in the thoracic spinal cord, has been homozygous for the *SOD1:c.118G>A* mutation, so there is little doubt that this mutation is closely associated with the disease. However, among the PWCs examined in this study, affected dogs were euthanized as a consequence of the disease as early as 12 years of age, whereas two of the seven unaffected PWCs were homozygous for this mutation and had not exhibited any of the clinical signs of DM or any spinal cord pathology by 13 to14 years of age. This indicates that there are other factors that determine whether a genetically predisposed dog develops DM or at least the age at which the disease develops. An understanding of the factors that modify the age of onset and rate of disease progression in DM may be useful in developing effective treatments for ALS.

DM as a disease model may serve as a valuable tool to investigate disease mechanisms, therapeutic strategies and disease markers for at least some forms of ALS. It is important to continue to thoroughly characterize DM, and develop outcome measures to provide biomarkers for reliable assessments of the efficacy of potential therapeutic interventions.

Acknowledgments

Special thanks to Cheryl A. Jensen for processing our nerve root and dorsal root ganglion samples, the MU Molecular Cytology Core for support with morphometric software analysis, Dr. Teresa E. Lever for her assistance in histological assessments, Alyssa C. Bujnak for her help with motor neuron and axon counting, and Dr. Michael Garcia for his assistance with data interpretation. The following general practitioners and veterinary specialists collected samples that were evaluated in this study: Drs. Michaela Cautela, Linda Downs, Conan Crocker, Sydney Moise, Eugene Garcia, Brad Peterson, Susan Carey, Bethany Russell, B Hortney, Chris Levine, John Calhoun, Bill Kieger, Gary Volk, Chris Roth, Tammy Stevenson, Marty Greer, Greg Leck, Kathleen Van Lanen, Todd Westbrook, Phil March, Brenda Perkins, Adam Moeser, and Shelley Newman.

Funding for this project was provided by the U.S. Department of Education's Graduate Assistance in Areas of National Need (GAANN) program, a College of Veterinary Medicine Phi Zeta Research Award, the University of Missouri Research Council Grant, University of Missouri MIZZOU Advantage, AKC Canine Health Foundation, and ALS Association.

References

Andersen PM, Forsgren L, Binzer M, Nilsson P, Ala-Hurula V, Keranen ML, Bergmark L, Saarinen A, Haltia T, Tarvainen I, Kinnunen E, Udd B, Marklund SL. Autosomal recessive adult-onset amyotrophic lateral sclerosis associated with homozygosity for Asp90Ala CuZn-superoxide dismutase mutation. A clinical and genealogical study of 36 patients. Brain. 1996; 119(Pt 4):1153–1172. [PubMed: 8813280]

Andersen PM, Nilsson P, Ala-Hurula V, Keranen ML, Tarvainen I, Haltia T, Nilsson L, Binzer M, Forsgren L, Marklund SL. Amyotrophic lateral sclerosis associated with homozygosity for an Asp90Ala mutation in CuZn-superoxide dismutase. Nat Genet. 1995; 10:61–66. [PubMed: 7647793]

Ausborn J, Wolf H, Stein W. The interaction of positive and negative sensory feedback loops in dynamic regulation of a motor pattern. Journal of Computational Neuroscience. 2009; 27:245–257. [PubMed: 19291377]

Averill DR Jr. Degenerative myelopathy in the aging German Shepherd dog: clinical and pathologic findings. J Am Vet Med Assoc. 1973; 162:1045–1051. [PubMed: 4196853]

Awano T, Johnson GS, Wade CM, Katz ML, Johnson GC, Taylor JF, Perloski M, Biagi T, Baranowska I, Long S, March PA, Olby NJ, Shelton GD, Khan S, O'Brien DP, Lindblad-Toh K, Coates JR. Genome-wide association analysis reveals a SOD1 mutation in canine degenerative myelopathy that resembles amyotrophic lateral sclerosis. Proc Natl Acad Sci U S A. 2009; 106:2794–2799. [PubMed: 19188595]

Braund KG, McGuire JA, Lincoln CE. Age-related changes in peripheral nerves of the dog. II. A morphologic and morphometric study of cross-sectional nerve. Vet Pathol. 1982; 19:379–398. [PubMed: 7090141]

Brooks BR, Miller RG, Swash M, Munsat TL. El Escorial revisited: revised criteria for the diagnosis of amyotrophic lateral sclerosis. Amyotroph Lateral Scler Other Motor Neuron Disord. 2000; 1:293–299. [PubMed: 11464847]

Charcot J-M JA. Deuxcas d'atrophie musculaire progressive avec lesions del substance grise et de faisceaux anterolateraux de moelle epiniere. Arch Phusiol Norm Pathol. 1869:354–357.

Coates JR, March PA, Oglesbee M, Ruaux CG, Olby NJ, Berghaus RD, O'Brien DP, Keating JH, Johnson GS, Williams DA. Clinical characterization of a familial degenerative myelopathy in Pembroke Welsh Corgi dogs. J Vet Intern Med. 2007; 21:1323–1331. [PubMed: 18196743]

Coates JR, Wininger FA. Canine degenerative myelopathy. Vet Clin North Am Small Anim Pract. 2010; 40:929–950. [PubMed: 20732599]

Dadon-Nachum M, Melamed E, Offen D. The “dying-back” phenomenon of motor neurons in ALS. J Mol Neurosci. 2011; 43:470–477. [PubMed: 21057983]

di Trapani G, David P, La Cara A, Servidei S, Tonali P. Morphological studies of sural nerve biopsies in the pseudopolyneuropathic form of amyotrophic lateral sclerosis. Clin Neuropathol. 1986; 5:134–138. [PubMed: 3720069]

Dyck PJ, Stevens JC, Mulder DW, Espinosa RE. Frequency of nerve fiber degeneration of peripheral motor and sensory neurons in amyotrophic lateral sclerosis. Morphometry of deep and superficial peroneal nerves. Neurology. 1975; 25:781–785. [PubMed: 1171412]

Fischer LR, Culver DG, Tennant P, Davis AA, Wang M, Castellano-Sanchez A, Khan J, Polak MA, Glass JD. Amyotrophic lateral sclerosis is a distal axonopathy: evidence in mice and man. Exp Neurol. 2004; 185:232–240. [PubMed: 14736504]

Forsberg K, Jonsson PA, Andersen PM, Bergemalm D, Graffmo KS, Hultdin M, Jacobsson J, Rosquist R, Marklund SL, Brannstrom T. Novel antibodies reveal inclusions containing non-native SOD1 in sporadic ALS patients. PLoS One. 2010; 5(7):e11552. [PubMed: 20644736]

Giannini F, Battistini S, Mancuso M, Greco G, Ricci C, Volpi N, Del Corona A, Piazza S, Siciliano G. D90A-SOD1 mutation in ALS: The first report of heterozygous Italian patients and unusual findings. Amyotroph Lateral Scler. 2010; 11:216–219. [PubMed: 20184519]

Griffiths IR, Duncan ID. Chronic degenerative radiculomyelopathy in the dog. J Small Anim Pract. 1975; 16:461–471. [PubMed: 1195675]

Guo YS, Wu DX, Wu HR, Wu SY, Yang C, Li B, Bu H, Zhang YS, Li CY. Sensory involvement in the SOD1-G93A mouse model of amyotrophic lateral sclerosis. Experimental & molecular medicine. 2009; 41:140–150. [PubMed: 19293633]

Heads T, Pollock M, Robertson A, Sutherland WH, Allpress S. Sensory nerve pathology in amyotrophic lateral sclerosis. Acta Neuropathol. 1991; 82:316–320. [PubMed: 1662002]

Hirano A. Cytopathology of amyotrophic lateral sclerosis. Adv Neurol. 1991; 56:91–101. [PubMed: 1649547]

Isaacs JD, Dean AF, Shaw CE, Al-Chalabi A, Mills KR, Leigh PN. Amyotrophic lateral sclerosis with sensory neuropathy: part of a multisystem disorder? J Neurol Neurosurg Psychiatry. 2007; 78:750–753. [PubMed: 17575021]

Katsuno M, Tanaka F, Adachi H, Banno H, Suzuki K, Watanabe H, Sobue G. Pathogenesis and therapy of spinal and bulbar muscular atrophy (SBMA). Progress in Neurobiology. 2012; 99:246–256. [PubMed: 22609045]

Kawamura Y, Dyck PJ, Shimono M. Morphometric comparison of the vulnerability of peripheral motor and sensory neurons in amyotrophic lateral sclerosis. Journal of Neuropathology and Experimental Neurology. 1981; 40:667–675. [PubMed: 7299423]

King AE, Dickson TC, Blizzard CA, Woodhouse A, Foster SS, Chung RS, Vickers JC. Neuron-glia interactions underlie ALS-like axonal cytoskeletal pathology. Neurobiology of Aging. 2011; 32:459–469. [PubMed: 19427060]

March PA, Coates JR, Abyad RJ, Williams DA, O'Brien DP, Olby NJ, Keating JH, Oglesbee M. Degenerative myelopathy in 18 Pembroke Welsh Corgi dogs. Vet Pathol. 2009; 46:241–250. [PubMed: 19261635]

Marcuzzo S, Zucca I, Mastropietro A, de Rosbo NK, Cavalcante P, Tartari S, Bonanno S, Preite L, Mantegazza R, P. B. Hind limb muscle atrophy precedes cerebral neuronal degeneration in G93A-SOD1 mouse model of amyotrophic lateral sclerosis: a longitudinal MRI study. Experimental Neurology. 2011; 231:30–37. [PubMed: 21620832]

Mentis GZ, Blivis D, Liu W, Drobac E, Crowder ME, Kong L, Alvarez FJ, Sumner CJ, O'Donovan MJ. Early functional impairment of sensory-motor connectivity in a mouse model of spinal muscular atrophy. Neuron. 2011; 69:453–467. [PubMed: 21315257]

Morgan BR, Coates JR, Johnson JC, Bujnak AC, Katz ML. Characterization of Intercostal Muscle Pathology in Canine Degenerative Myelopathy: A Disease Model for Amyotrophic Lateral Sclerosis. J Neuroscience Res. 2013 In press.

Mulder DW, Bushek W, Spring E, Karnes J, Dyck PJ. Motor neuron disease (ALS): evaluation of detection thresholds of cutaneous sensation. Neurology. 1983; 33:1625–1627. [PubMed: 6685835]

Ogawa M, Uchida K, Park ES, Kamishina H, Sasaki J, Chang HS, Yamato O, Nakayama H. Immunohistochemical observation of canine degenerative myelopathy in two Pembroke Welsh Corgi dogs. J Vet Med Sci. 2011; 73:1275–1279. [PubMed: 21628865]

Ogawa M, Uchida K, Yamato O, Inaba M, Uddin MM, Nakayama H. Neuronal Loss and Decreased GLT-1 Expression Observed in the Spinal Cord of Pembroke Welsh Corgi Dogs With Canine Degenerative Myelopathy. Vet Pathol. 2013 in press.

Pugdahl K, Fuglsang-Frederiksen A, de Carvalho M, Johnsen B, Fawcett PR, Labarre-Vila A, Liguori R, Nix WA, Schofield IS. Generalised sensory system abnormalities in amyotrophic lateral sclerosis: a European multicentre study. J Neurol Neurosurg Psychiatry. 2007; 78:746–749. [PubMed: 17575020]

Redler RL, Dokholyan NV. The complex molecular biology of amyotrophic lateral sclerosis (ALS). Progress in Molecular Biology & Translational Science. 2012; 107:215–262. [PubMed: 22482452]

Schaefer AM, Sanes JR, Lichtman JW. A compensatory subpopulation of motor neurons in a mouse model of amyotrophic lateral sclerosis. J Comp Neurol. 2005; 490:209–219. [PubMed: 16082680]

Shelton GD, Johnson GC, O'Brien DP, Katz ML, Pesayco JP, Chang BJ, Mizisin AP, Coates JR. Degenerative myelopathy associated with a missense mutation in the superoxide dismutase 1 (SOD1) gene progresses to peripheral neuropathy in Pembroke Welsh Corgis and Boxers. J Neurol Sci. 2012; 318:55–64. [PubMed: 22542607]

Shi P, Gal J, Kwinter DM, Liu X, Zhu H. Mitochondrial dysfunction in amyotrophic lateral sclerosis. Biochimica et Biophysica Acta. 2010; 1802:45–51. [PubMed: 19715760]

Sobue G, Hashizume Y, Mitsuma T, Takahashi A. Size-dependent myelinated fiber loss in the corticospinal tract in Shy-Drager syndrome and amyotrophic lateral sclerosis. Neurology. 1987; 37:529–532. [PubMed: 3822153]

Sobue G, Matsuoka Y, Mukai E, Takayanagi T, Sobue I, Hashizume Y. Spinal and cranial motor nerve roots in amyotrophic lateral sclerosis and X-linked recessive bulbospinal muscular atrophy: morphometric and teased-fiber study. Acta Neuropathol. 1981; 55:227–235. [PubMed: 6891550]

Sunico CR, Dominguez G, Garcia-Verdugo JM, Osta R, Montero F, Moreno-Lopez B. Reduction in the motoneuron inhibitory/excitatory synaptic ratio in an early-symptomatic mouse model of amyotrophic lateral sclerosis. Brain Pathology. 2011; 21:1–15. [PubMed: 20653686]

Tanaka F, Ikenaka K, Yamamoto M, Sobue G. Neuropathology and omics in motor neuron diseases. [Review]. Neuropathology. 2012; 32:458–462. [PubMed: 22187969]

Vucic S, Stein TD, Hedley-Whyte ET, Reddel SR, Tisch S, Kotschet K, Cros D, Kiernan MC. FOSMN syndrome: novel insight into disease pathophysiology. Neurology. 2012; 79:73–79. [PubMed: 22722633]

Wong M, Martin LJ. Skeletal muscle-restricted expression of human SOD1 causes motor neuron degeneration in transgenic mice. Human Molecular Genetics. 2010; 19:2284–2302. [PubMed: 20223753]

Zhou J, Yi J, Fu R, Liu E, Siddique T, Rios E, Deng HX. Hyperactive intracellular calcium signaling associated with localized mitochondrial defects in skeletal muscle of an animal model of amyotrophic lateral sclerosis. Journal of Biological Chemistry. 2010; 285:705–712. [PubMed: 19889637]

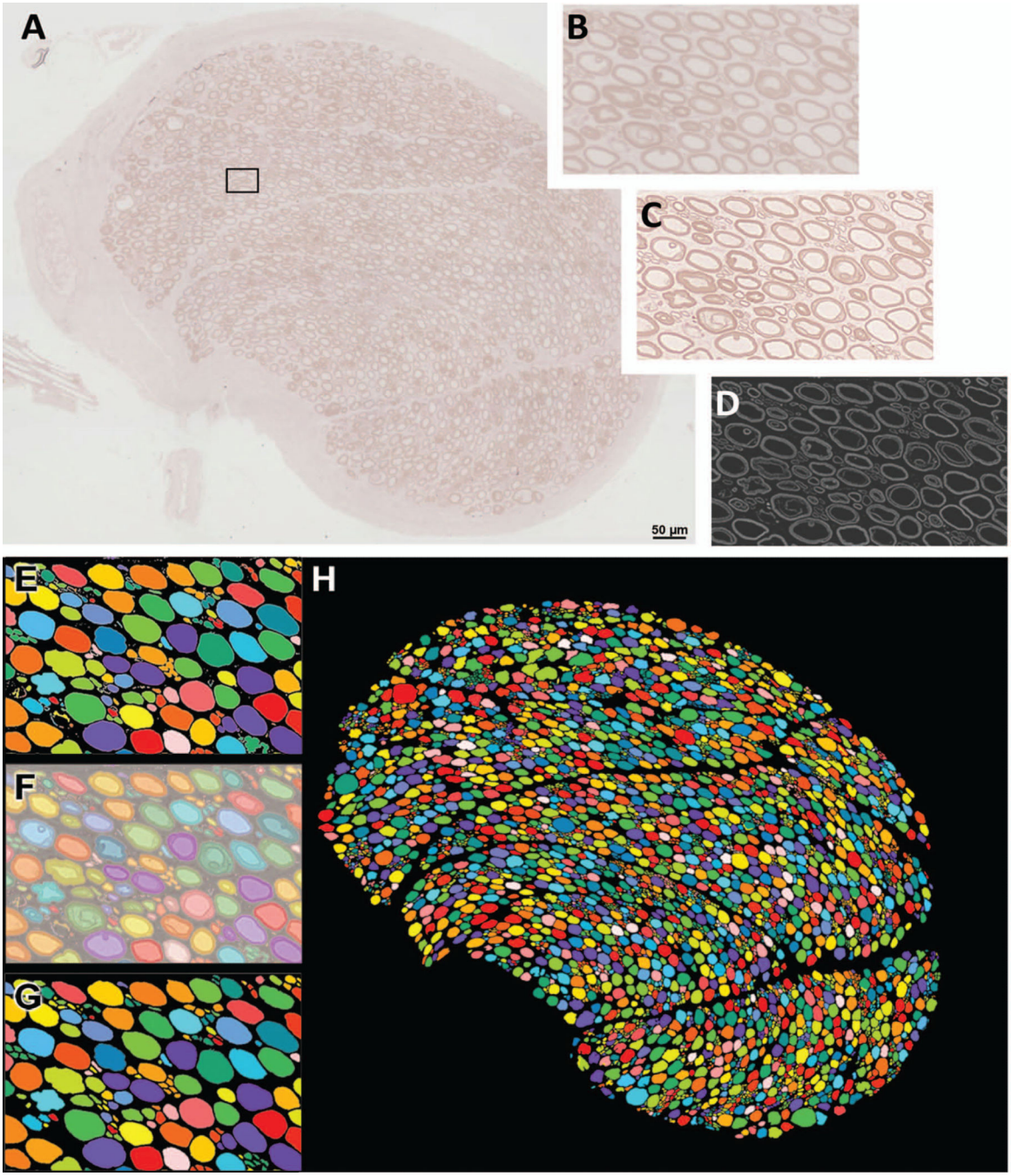

Figure 1.

Procedure for obtaining morphometric measurements in T8 motor root cross-sections. (A) Resin embedded nerves were sectioned and stained with P-phenylene diamine (PPD), imaged using light microscopy, and composite images of the entire nerve cross-sections were constructed. (B) Magnified image of area outlined in (A). (C) Images were sharpened using Photoshop™ tools. (D) Imaris® software was used to invert the image, and remove background noise. (E) Multicolored image produced by the automated count tool in MetaMorph® software. Colors indicate what software distinguishes as individual objects.

Note that several adjacent axons are being mistaken for a single object. (F) Manual corrections were made in Photoshop by overlaying, and increasing the transparency of, the multicolored image over the sharpened light micrograph. (G) Multicolored images after manual corrections. (H) Corrected multicolored image of entire nerve root cross-section. (Illustration represents a T8 motor root cross section).

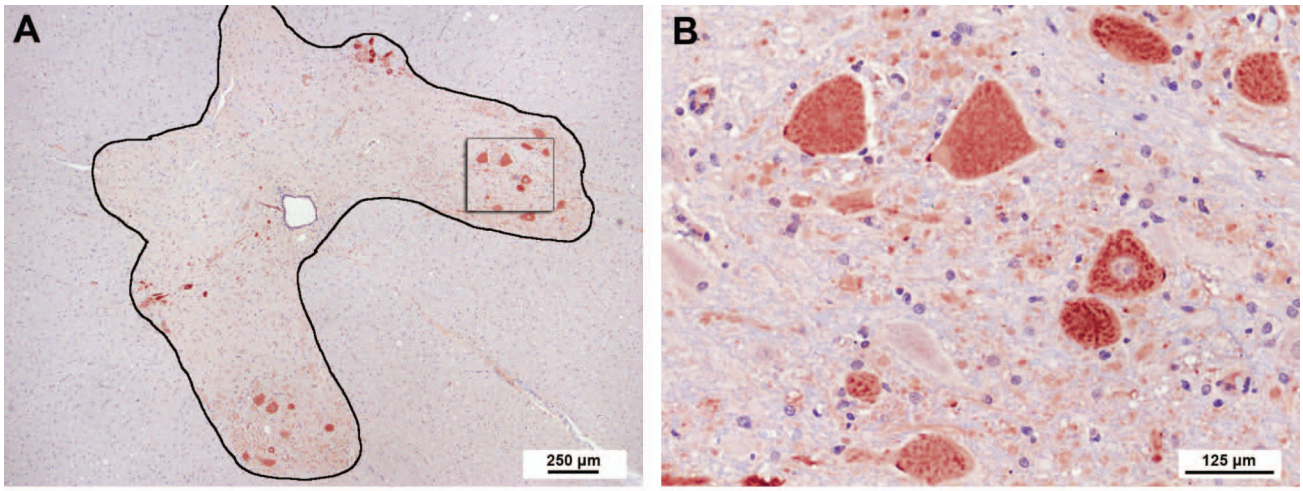

C

		Cross Sectional Area (µm²)			
PWC	# of Dogs	Mean	Standard Deviation	Range	Density (# of cells/section)
Unaffected	5	724.21 ± 145.11	424.30 ± 41.17	1,920.82 ± 320.10	13 ± 1
Affected	8	838.48 ± 200.03	516.79 ± 72.92	2,154.93 ± 381.23	15 ± 4
P-Value		0.29	0.02 *	0.27	0.17
Boxer					
Unaffected	3	467.81 ± 226.64	308.23 ± 151.36	1,257.43 ± 590.91	18 ± 4
Affected	7	438.68 ± 46.20	305.29 ± 33.42	1,240.24 ± 169.38	22 ± 4
P-Value		1	0.83	0.83	0.30

Figure 2.

Thoracic motor neuron morphometric measurements. (A, B) T7 spinal cord section from an unaffected 9 year old Boxer stained with ChAT. (B). Higher magnification of highlighted box within Rexed lamina 9 in A. This image is a representation of the normal motor neuron morphology seen in unaffected and affected dogs of both breeds. (C) Morphometric measurements obtained from PWC (top) and Boxers (Bottom). Pooled data indicate no difference in the motor neuron density between unaffected and affected samples of either breed (Affected boxers: one grade 1, three grade 2, one grade 3, and two grade 4 dogs; Affected PWC: two grade 2, two grade 3, and four grade 4 dogs). Likewise no differences were seen in the mean soma cross sectional area (CSA) or size range. In PWC's a significant difference was seen in the CSA standard deviation, suggesting more variability in soma area in affected dogs (p=0.02). One Way ANOVA indicated the difference in standard deviation is attributed to a significant difference between unaffected and late stage (grade 3-4) PWC samples (p= 0.04).

A

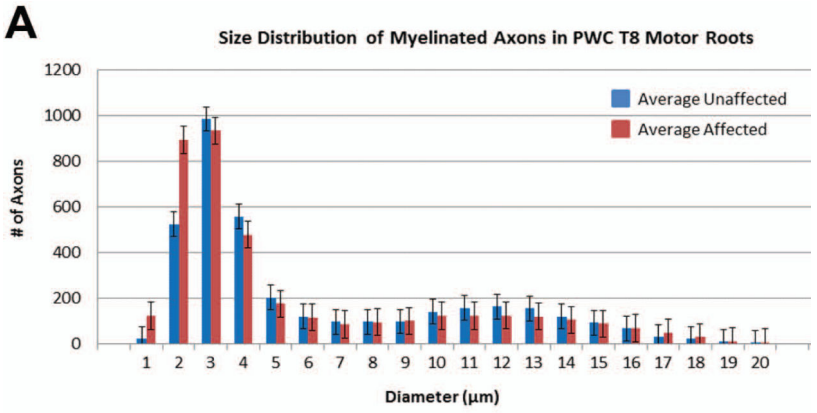

B

PWC	Unaffected	Affected	P value
% of axons ≤ 5 µm	62.30%	64.47%	0.87
% of axons > 5 µm	37.70%	32.53%	0.52
Average # of axons ≤ 5 µm	2,086 ± 268	2,427 ± 593	0.25
Average # of axons > 5 µm	1,587 ± 253	1,430 ± 151	0.18

C

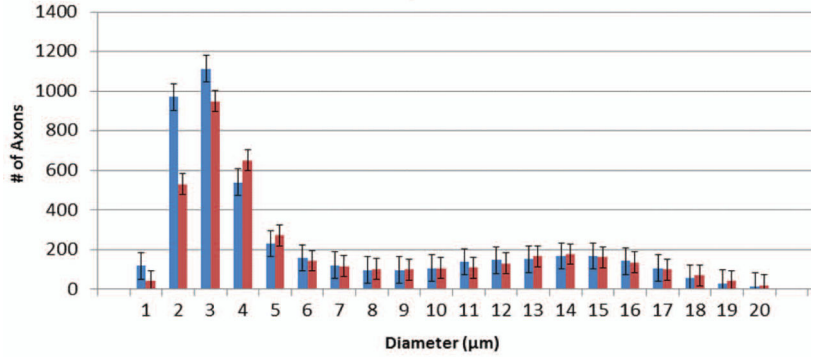

D

Boxers	Unaffected	Affected	P value
% of axons ≤ 5 µm	63.32 %	59.08%	0.89
% of axons > 5 µm	36.68%	40.92%	0.52
Average # of axons ≤ 5 µm	2,954 ± 671	2,445 ± 807	0.30
Average # of axons > 5 µm	1,765 ± 283	1,708 ± 376	0.79

Figure 3.

Motor root myelinated axon diameter distribution from PWC's (A,B) and Boxers (C,D). Histograms show a bimodal size distribution with one peak representing small caliber axons, and one peak representing large caliber axons (A, C). For both breeds, no obvious differences could be seen between large caliber axons from control and affected motor roots, while the small caliber peak was more variable. (B, D) For both breeds, no statistical difference was seen in the percentage or average numbers of axons ≤5 µm >. Data represented in this figure were obtained from the same samples depicted in Tables IV and V.

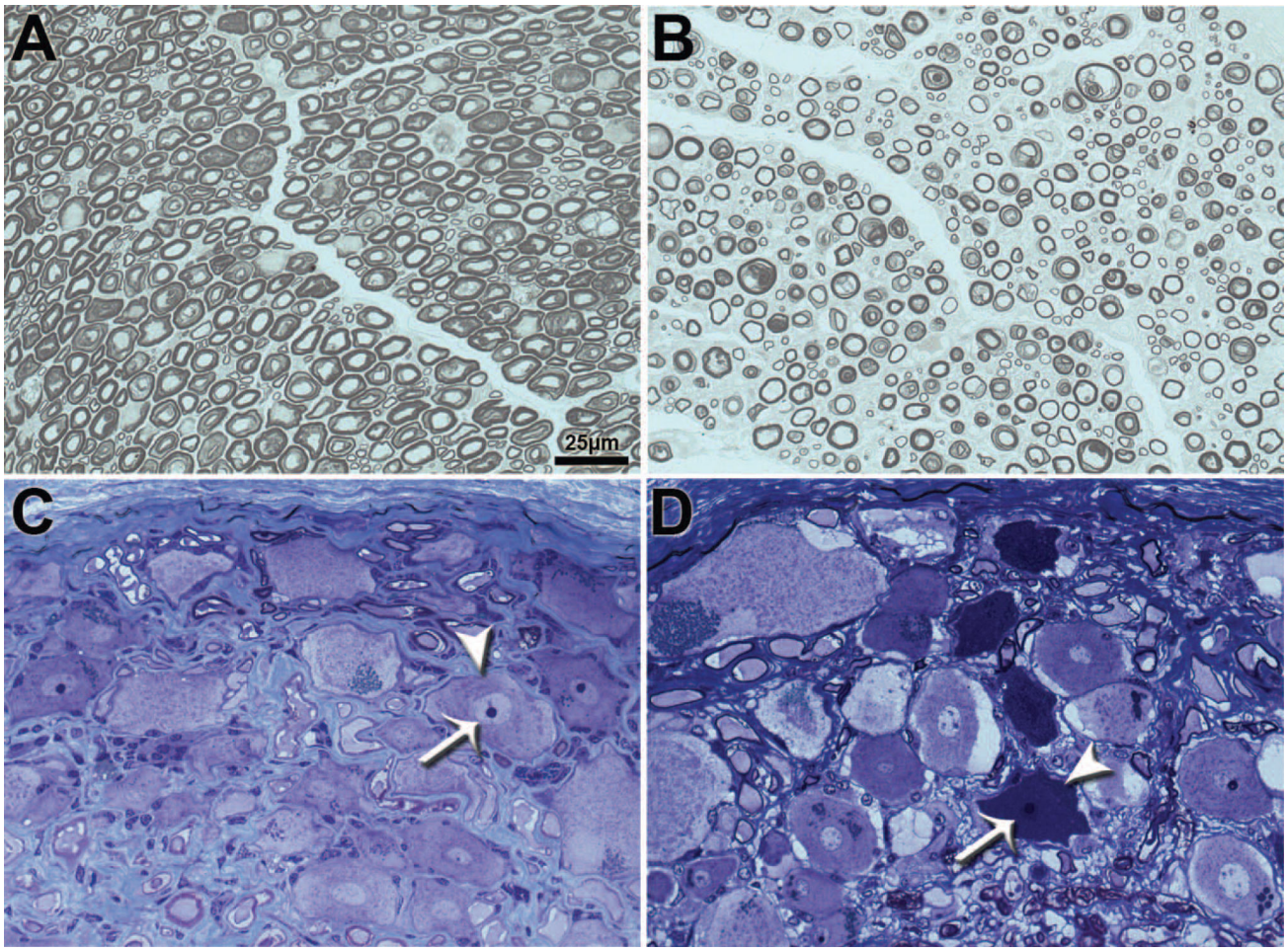

Figure 4.

Histological sections of T8 sensory roots (A and B) and dorsal root ganglia (DRG) (C and D) in PWC samples. EM-fixed sensory roots and DRG from control (A,C) and grade 4 (B,D) PWC samples were embedded in resin and stained with PPD and toluidine blue respectively. Compared to controls (A), sensory roots from grade 4 PWC (B) exhibited decreased myelinated axon density. DRG neurons from grade 4 PWC (D) contained numerous cells with condensed cytoplasm (arrowhead) and severely pyknotic nuclei (arrow) that were not present in the DRG neurons from age-matched control dogs (arrowhead and arrow in C denote cytoplasm and nucleus of normal neuron for comparison).

A

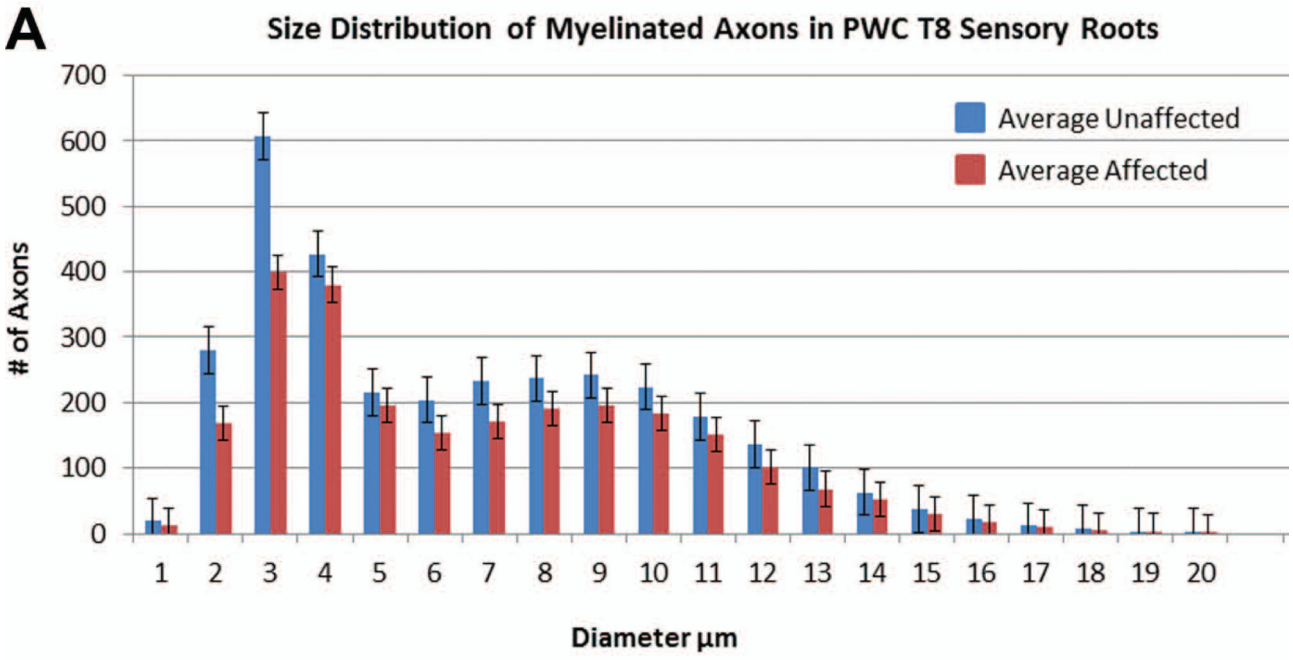

B

PWC	Unaffected	Affected	P value
% of axons ≤ 5 µm	47.53%	46.28 %	0.95
% of axons > 5 µm	52.29%	53.60 %	0.98
Average # of axons ≤ 5 µm	1,550 ± 345	1,156 ± 168	**0.03***
Average # of axons > 5 µm	1,711 ± 266	1,341 ± 242	**0.03***

Figure 5.

PWC sensory root myelinated axon diameter distribution. (A)Histogram shows a bimodal size distribution with one peak representing small caliber axons, and one peak representing large caliber axons. (B) There was a statistically significant difference in the average number of axons ≤5 µm (p= 0.03) and >5 µm (p=0.03). Data represented in this figure were obtained from the same samples depicted in Table VI.

Table I

Summary of the number of dogs within each disease grade*

	Numbers of dogs in each grade				
Breed	**Control**	**Grade 1**	**Grade 2**	**Grade 3**	**Grade 4**
PWC	7	0	5	4	6
Boxer	6	3	3	2	1

* See Table III for definitions of disease grades

Table II

SOD1 Genotypes. DM is associated with a *SOD1:c.118G>A* mutation. Homozygosity for the A allele is a risk factor for developing DM in Boxers and PWCs.

	Number of Dogs of Each *SOD1* Genotype (age in years)		
Disease Status - Breed	G/G	A/G	A/A
Unaffected PWC	1 (16)	4 (13-17)	2 (13-14)
Affected PWC	0	0	15 (12-15)
Unaffected Boxer	0	4 (8-12)	2 (9)
Affected Boxer	0	0	9 (10-12)

Table III

Clinical grading scale of disease progression in DM affected dogs.

Clinical Grade	Clinical Signs*
1	**Paraparesis and General Proprioceptive Ataxia**
	• Progressive general proprioceptive ataxia
	• Asymmetric and spastic paraparesis
	• Postural reaction deficits in pelvic limb
	• Intact spinal reflexes (patellar reflex may be decreased)
2	**Nonambulatory Paraparesis to Paraplegia**
	• Mild to moderate loss of muscle mass in pelvic limbs
	• Reduced to absent spinal reflexes in pelvic limbs
	• +/- urinary and fecal incontinence
3	**Paraplegia to Thoracic Limb Weakness**
	• Signs of thoracic limb weakness
	• Flaccid paraplegia
	• Absence of spinal reflexes in pelvic limbs
	• Severe loss of muscle mass in pelvic limbs
	• Urinary and fecal incontinence
4	**Tetraplegia and Brain Stem Signs**
	• Flaccid tetraplegia
	• Difficulty with swallowing and tongue movements
	• Absence of spinal reflexes in all limbs
	• Reduced to absent cutaneous trunci reflex
	• Generalized and severe loss of muscle mass
	• Urinary and fecal incontinence

* The presumptive diagnosis of DM for dogs was based on the presence and progression of these signs. Early stages include grades 1-2, and late stages include grades 3-4. (Adapted from (Coates and Wininger 2010); Shelton et al 2012)

Table IV

PWC T8 motor root morphometric measurement results from 5 unaffected and 8 affected *(four grade 2, one grade 3, and three grade 4)* dogs.

PWC T8 Motor Roots	Unaffected	Affected	P value
Number of dogs	5	8	
Average count of axons	3,676 ± 262	3,863 ± 691	0.57
Average endoneural CSA* (μm^2)	308,081.54 ± 39,460.49	297,826.80 ± 55,818.72	0.72
Average area occupied by axons (μm^2)	191,114.56 ± 35,453	179,168.71 ± 24,679.03	0.48
% of endoneural area occupied by axons	61.7% ± 6.1%	60.7 ± 5.8%	0.78
Average axon density count/mm^2)	12,165.08 ± 2,131	13,400.49 ± 3,874.93	0.53

*CSA = Cross sectional area

Table V

Boxer T8 motor root morphometric measurement results from 5 unaffected and 8 affected (two grade 1, three grade 2, one grade 3, and two grade 4) dogs.

Boxer T8 Motor Roots	Unaffected	Affected	P value
Number of dogs	5	8	
Average count of axons	4,697 ± 827	4,140 ± 1,104	0.35
Average endoneural CSA* (μrn^2)	443,654.10 ± 94,990.21	464,871.30 ± 124,963.56	0.75
Average area occupied by axons (μm^2)	267,532.55 ± 69,695.82	269,769.55 ± 62814.24	0.95
% of endoneural area occupied by axons	60.3 % ± 8.5%	59.1% ± 9.8%	0.83
Average axon density (count/mm^2)	10,850.21 ± 2,368.04	9,039.09 ± 2,143.59	0.22

*CSA = Cross sectional area

Table VI

PWC Morphometric Sensory Root Data *(affected samples: two grade 3, four grade 4)*

PWC T8 Sensory Roots	Unaffected	Affected	P value
number of dogs	6	6	
Average count of axons	3,261 ± 354	2,498 ± 324	**0.003***
Average endoneural CSA* (μm^2)	299,035.80 ± 51,135.46	287,306.10 ± 104,376.02	0.81
Average area occupied by axons (μm^2)	168,275.15 ± 50,113.15	131,682.17 ± 28,538.90	0.15
% of endoneural area occupied by axons	56.9% ± 15.1%	48.2 ± 9.5%	0.26
Average axon density (count/mm^2)	11,078.84 ± 1,663.80	9,606.45 ± 3,192.25	0.34

* CSA = Cross sectional area